The Astrophysical Journal Supplement Series, 142:285–293, 2002 October

BLUE LINES AS CHROMOSPHERIC DIAGNOSTICS: THE Al I LINES AT 3944 AND 3961 Å

Pablo J. D. Mauas,[1] Roberto Fernández Borda, and María Luisa Luoni
Instituto de Astronomía y Física del Espacio, IAFE, CC. 67 Suc. 28, 1428 Buenos Aires, Argentina; pablo@iafe.uba.ar
Received 2002 January 2; accepted 2002 May 30

ABSTRACT

We present a simple atomic model for the synthesis of the Al I resonance lines, near the Ca II H and K lines. We study whether the computed profiles are influenced by the choice of the atomic parameters and find that, although several cross sections are not known accurately, the line profiles do not depend on them and are therefore useful as diagnostics of the atmospheric structure.

We study which transitions need not to be included in the model, in order to reduce as much as possible the computing time. We compare the profiles computed for a standard model of the quiet solar atmosphere with the observations and find very good agreement.

We found that the inclusion of the proper line-blanketing opacity is fundamental for an accurate calculation of the ionization balance and that irradiation by UV lines originating in the transition region does not affect the Al I emission.

Subject headings: atomic processes — line: formation — line: profiles — stars: chromospheres — Sun: chromosphere

1. INTRODUCTION

One of the most observed regions of solar and stellar spectra is the one of the Ca II H and K lines, at 3933 and 3968 Å, since these lines are the most widely used indicators of chromospheric activity, both in the Sun and in other cool stars. In many cases, the Ca lines are used to construct semiempirical models of the stellar atmosphere, as a way to determine the structure of the chromosphere.

For "semiempirical" we mean that the atmospheric structure is adjusted to find a satisfactory match between the observations in several spectral features and the predictions of the model. To avoid indeterminations in the models, a number of lines as large as possible should be included in the process. Therefore, the study of other lines in the Ca II spectral region can help to obtain better constrained models.

However, to include any particular line in the modeling it is necessary to build an accurate atomic model, compiling the available atomic data, computing the parameters not available in the literature, and checking how much influence the possible inaccuracies in these parameters might have on the computed atmospheric model.

In a recent paper, Cincunegui & Mauas (2001, hereafter CM01) studied two lines of Si I at 3905 and 4103 Å and found that, although several cross sections are not known accurately, the line profiles do not depend strongly on them and are therefore useful as diagnostics of the atmospheric structure. They compared the profiles computed for a standard model of the quiet solar atmosphere with the observations and found very good agreement.

CM01 also found that irradiation by UV lines originating in the transition region above sunspot umbra or plages strongly enhances the continuum between 1300 and 1700 Å, which is due to Si I bound-free transitions, and that if line fluxes typical of the impulsive phase of flares is assumed, the line profiles are also affected.

Observations of the Si I line at 3905 Å were used by Falchi & Mauas (2002) to build semiempirical models of the solar chromosphere for five different times during the evolution of a solar flare, together with the profiles of the Ca II K line and Hδ, using spectra obtained by Cauzzi et al. (1995) with the Universal Spectrograph (USG) at the Vacuum Tower Telescope of the National Solar Observatory, Sacramento Peak, in the range 3500–4200 Å.

The main interest of the work by Falchi & Mauas (2002) was to study the velocity fields induced by the flare, and the Si I line proved very useful in this respect since it is much narrower, and it is formed in a region of the chromosphere better determined than the calcium and hydrogen lines.

Other strong lines in the spectral region of interest are the Al I resonance lines at 3944 and 3961 Å, which lie in the wings of the Ca II lines. These lines are observed in emission in the spectra obtained by Cauzzi et al. (1995). The profile of the 3961 Å line was mentioned as a stellar activity indicator by Linsky et al. (1979).

To our knowledge, the only work studying the formation of the Al I lines in solar and stellar atmospheres is the one by Baumüller & Gehren (1996, hereafter BG96; see also Baumüller & Gehren 1997), who were mainly interested in the determination of Al abundance in cool metal-poor stars. For that reason, they made a number of simplifications appropriate for the study of weak photospheric lines, but inadequate for activity studies. In particular, they made their calculations for a solar model with no chromospheric rise, clearly neglecting all type of activity. This approximation turned out to be good for the weaker lines, but it cannot be applied to the resonance lines of interest here, which are formed in the chromosphere.

In this paper we build an atomic model adequate to compute the profiles of the resonance lines of Al I and study how the indetermination in the atomic parameters can affect the results. Since it will be used to compute atmospheric models with velocity fields, we study which is the smallest number of levels and transitions that still retains all the important physics. We do so in order to reduce the computing time, since when velocity is included in the radiative transfer

[1] Member of the Carrera del Investigador Científico, CONICET, Argentina.

equations the number of frequency points at which the calculations have to be done is multiplied by the number of height points in the grid, and therefore the computing time increases by a large factor.

In § 2 we discuss the atomic parameters available in the literature. In § 3 we study the effect of the different levels on the ionization equilibrium and on the emitted profiles. In § 4 we present the "optimum model," i.e., the one that includes all the important processes, with the smallest number of transitions. In § 5 we check how much the computed profiles change when the atomic parameters are modified, to estimate the reliability of our atomic model. In § 6 we study the influence that the irradiation by ultraviolet lines coming down from the transition region has on the profiles. Finally, in § 7 we discuss the results.

TABLE 1

Atomic Parameters for Bound-Free Transitions

l	Designation	λ_l (Å)	g_l	α_0 (Mb)	Ω_l (cm^3 s^{-1})
1.....	$3p\ ^2P^o_{1/2}$	2071	2	60.90	6.5(−8)
2.....	$3p\ ^2P^o_{3/2}$	2077	4	60.90	6.5(−8)
3.....	$4s\ ^2S$	4361	2	0.18	4.1(−9)
4.....	$3p^2\ ^4P$	5205	12	36.60	1.0(−8)
5.....	$3d\ ^2D$	6312	10	30.30	2.2(−7)
6.....	$4p\ ^2P^o$	6524	6	17.50	9.3(−8)
7.....	$5s\ ^2S$	9443	2	1.71	1.0(−8)
8.....	$nd\ ^2D$	10696	10	10.10	1.0(−8)
9.....	$5p\ ^2P^o$	12490	6	18.40	1.0(−8)
10.....	$4f\ ^2F^o$	14369	14	31.15	1.0(−8)
11.....	$6s\ ^2S$	16302	2	4.49	1.0(−8)

2. ATOMIC PARAMETERS

We have used an atomic model including 11 levels and 22 radiative transitions, which is shown in Figure 1. In Table 1 we list the designation and ionization wavelength of each level, together with the ionization rates discussed below. Note that the two lowest levels belong to the same term, $3P\ ^2P^o$. These are the lowest levels of the lines under study, and we split them in order to treat accurately the different opacities, which are due to the wings of the Ca II lines.

BG96, who were interested in transitions connecting higher levels, used a model including 51 terms, describing the complete doublet system with $n \leq 10$. Since the lines we are interested in correspond to transitions between the three lowest levels, we believe that this model should be complete enough and that it should include all the levels and transitions needed to compute the populations of the lowest levels. However, we tested this assessment computing the line profiles and the populations of these levels with a 25 level atom, including 71 more radiative transitions, which are shown as dotted in Figure 1. We will return to this point in § 3.

As far as we know, there is very little work done to study the relevant atomic parameters of Al I. Therefore, the problem of constructing a reliable model of the atom, which is usually hard, is harder in this case. However, the lines under study are the resonant lines of this system, a fact that simplifies the model and reduces the number of levels and transitions relevant for this study.

For the solar Al I abundance, we use 2.951×10^{-6}, or, in the usual logarithmic scale where the abundance of hydrogen is set to 12, a value of 6.47, as given by Grevesse et al. (1991).

In this section we present the atomic data we have used and discuss their uncertainties.

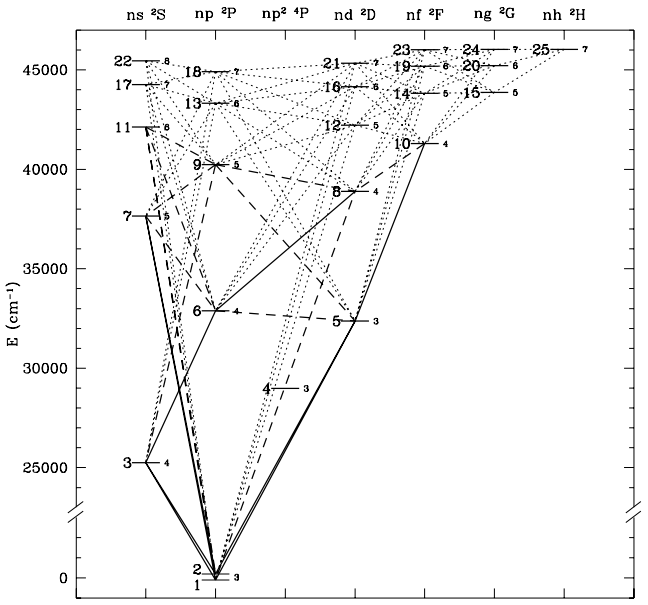

Fig. 1.—Energy level diagram of the atomic model. The solid lines indicate radiative transitions between the levels included in the optimum model, and dashed lines indicate transitions included only in the complete model. The levels from 12 to 25 and the transitions shown as dotted lines have been included to check whether additional terms have influence on the resonance lines profiles (see § 3).

2.1. *Bound-Free Cross Sections*

To study whether, as in the case of Si I (see CM01), the ionization balance of Al I is strongly affected by the transition region UV lines irradiating the low chromosphere and $T_{\min}$ region, very accurate photoionization cross sections are needed. In particular, autoionization resonances can be fundamental to determine the Al I populations. In this paper we use the theoretical cross sections by Mendoza et al. (2002), as given by the TOPbase database at the CDS (Cunto et al. 1993). These rates are similar to the ones used by BG96 (see their Fig. 2).

The values at threshold are listed in Table 1. For levels 1 and 2 these values are similar to the experimental values by Kohl & Parkinson (1973), and by Roig (1975). For level 3, Dragon & Mutschlecner (1980) give a value of 1.22Mb, based on the theoretical calculations by Peach (1970).

The collisional ionization rate per atom in level l is given by

$$C_{lk} = n_e \Omega_l(T) \exp(-h\nu_{kl}/kT) \ . \qquad (1)$$

The adopted values for $\Omega_l(T)$ at 5000 K are listed in Table 1. For the first six levels, we use the values adopted by Vernazza et al. (1976; E. H. Avrett 1989, private communication), and for the remaining ones we use a constant value of 10^{-8} cm^3 s^{-1} , which can be considered as an order of magnitude estimate. As the collisional ionization and

recombination rates are much smaller than the corresponding radiative rates, we believe that it is not necessary to use more accurate data.

2.2. *Bound-Bound Cross Sections*

We considered all the allowed transitions between the 11 levels of our atomic model. For the Einstein coefficient A_{ul} we adopted the values of the NIST compilation,[2] when available, since this is a critical compilation of the best values available in the literature.

For the remaining transitions, we adopted the experimental values by Buurman et al. (1986) or the ones given by the TOPbase database. These values are listed in Table 2, with the corresponding reference. In general, the values given by different authors do not differ by more than 10%, except for the forbidden transitions, which are not important for the statistical equilibrium of the atom.

The value of the Einstein coefficients of the resonance lines are of particular importance for the present study. Unlike for other atoms, there are not many studies of this parameter. The NIST value adopted here, of 4.93×10^7 s^{-1}, agrees well with the values given by Morton (1991) and TOPbase, of 4.86 and 5.27×10^7 s^{-1}.

Also shown in Table 2 are line half-widths at half-maximum for radiative ($C_{\rm rad}$), Van der Waals ($C_{\rm VdW}$), and Stark ($C_{\rm Stk}$) broadening. We assume that the absorption coefficient for each line has a Voigt profile given by

$$\phi_\nu = \frac{a}{\pi^{3/2}\Delta\nu_{\rm D}} \int_{-\infty}^{\infty} \frac{e^{-x^2}\,dx}{a^2 + [x - (\nu - \nu_0)/\Delta\nu_{\rm D}]^2}\ , \qquad (2)$$

where $\Delta\nu_{\rm D}$ is the Doppler width, and a is the Voigt parameter

$$a = \left[C_{\rm rad} + C_{\rm VdW}\left(\frac{n_{\rm H\,I}}{10^{16}}\right)\left(\frac{T}{5000}\right)^{0.3} + C_{\rm Stk}\left(\frac{n_e}{10^{12}}\right)\right] \Big/ \Delta\lambda_{\rm D}\ . \qquad (3)$$

Here $n_{\rm H\,I}$ and n_e are the atomic hydrogen and electron densities, T is the electron temperature, and the Doppler width $\Delta\lambda_{\rm D} = (\lambda/\nu)\Delta\nu_{\rm D}$ is in Å units.

We have calculated $C_{\rm rad}$ according to Mihalas (1970). The Stark parameters were taken from the Vienna Atomic Line Database (VALD, Kupka et al. 1999; Ryabchikova et al. 1999; Piskunov et al. 1995). These values were taken, in turn, from Kurucz's compilation of atomic data on CD-ROM.

Röndings & Kush (1978) publish experimental values for the Stark broadening of the 3–1, 3–2, 5–1, and 5–2 lines of our models. Their values agree between 10% with the VALD values used here. As will be discussed in § 5.4, these differences would have no effect on the computed profiles.

The Van der Waals half-widths were taken from calculations by Anstee & O'Mara (1995) for the *s–p* and *p–s* transitions, including the resonance lines, and from Barklem & O'Mara (1997) and Barklem, O'Mara, & Ross (1998b) for the remaining ones (see also Barklem, Anstee, & O'Mara

[2] Wiese, W. L., & Fuhr, J. R. 1999, NIST Atomic Spectra Database, National Institute of Standards and Technology (http://physics.nist.gov).

TABLE 2
Atomic Parameters for Radiative Bound-Bound Transitions

Line	A_{ul} (s^{-1})	λ (Å)	$C_{\rm rad}$ (Å)	$C_{\rm VdW}$ (Å)	$C_{\rm Stk}$ (Å)	Ω_{lu} (cm^3 s^{-1}) 3000 K	5000 K	8000 K	$\Omega^{\rm H}_{lu}$ (cm^3 s^{-1}) 5000 K
3–1	4.93(7)[a]	3944	6.1(−5)	1.56(−4)	1.8(−6)	2.2(−08)	2.7(−08)	2.7(−08)	3.0(−14)
5–1	2.52(7)[a]	3082	1.2(−5)	8.33(−5)	2.5(−6)	2.3(−08)	2.7(−08)	3.0(−08)	5.3(−14)
7–1	1.33(7)[a]	2652	9.1(−6)	1.38(−4)	4.4(−6)	1.5(−09)	1.5(−09)	1.8(−09)	5.7(−15)
8–1*	9.20(6)[a]	2567	6.6(−6)	1.39(−4)	4.8(−6)	4.5(−09)	4.6(−09)	5.7(−09)	2.5(−14)
11–1*	4.78(6)[a]	2372	3.0(−6)	9.08(−5)		3.5(−10)	3.5(−10)	4.4(−10)	3.5(−15)
3–2	9.80(7)[a]	3961	6.1(−5)	1.56(−4)	1.8(−6)	2.2(−08)	2.7(−08)	2.7(−08)	1.5(−14)
5–2	4.92(7)[a]	3092	1.9(−5)	8.33(−5)	2.5(−6)	2.3(−08)	2.7(−08)	2.9(−08)	2.7(−14)
7–2	2.64(7)[a]	2660	9.2(−6)	1.38(−4)	4.4(−6)	1.5(−09)	1.5(−09)	1.9(−09)	2.9(−15)
8–2*	1.86(7)[a]	2575	6.7(−6)	1.39(−4)	4.8(−6)	4.6(−09)	4.6(−09)	5.8(−09)	1.3(−14)
11–2*	9.50(6)[a]	2378	3.7(−6)	9.08(−5)		3.6(−10)	3.6(−10)	4.4(−10)	1.8(−15)
6–3	1.82(7)[a]	13141	7.6(−4)	2.17(−3)	8.0(−5)	2.1(−06)	2.2(−06)	2.5(−06)	1.6(−11)
9–3*	1.69(6)[a]	6696	1.8(−4)	1.18(−3)	5.3(−5)	1.8(−08)	1.7(−08)	1.9(−08)	8.5(−13)
6–5*	2.50(3)[c]	190733	9.0(−2)	4.00(−1)		1.2(−06)	1.3(−06)	1.3(−06)	1.1(−6)
9–5*	1.31(5)[b]	12750	3.4(−4)	3.67(−3)	1.3(−5)	2.6(−09)	2.9(−09)	3.2(−09)	2.9(−12)
10–5	1.78(7)[a]	11257	3.2(−4)	2.88(−3)	7.4(−7)	5.3(−07)	5.9(−07)	6.4(−07)	3.9(−12)
7–6*	9.00(6)[b]	21120	8.0(−4)	1.21(−2)	2.2(−4)	6.4(−07)	7.2(−07)	8.4(−07)	1.6(−11)
8–6	1.01(7)[a]	16750	4.2(−4)	4.88(−3)	1.5(−4)	1.6(−06)	1.7(−06)	1.8(−06)	2.7(−11)
11–6*	3.30(6)[a]	10877	1.2(−4)	6.96(−3)	2.7(−4)	2.1(−08)	2.3(−08)	2.5(−08)	8.0(−13)
9–7*	2.80(6)[b]	38622	2.1(−3)	4.46(−2)	2.1(−4)	1.7(−05)	2.1(−05)	2.2(−05)	2.4(−9)
9–8*	4.10(5)[b]	74390	6.3(−3)	1.14(−1)	1.3(−3)	6.3(−06)	6.4(−06)	7.1(−06)	1.1(−8)
10–8*	2.50(6)[c]	41900	2.7(−3)	3.38(−2)	6.2(−4)	9.2(−06)	1.2(−05)	1.2(−05)	1.6(−9)
11–9*	2.78(6)[c]	53390	1.9(−3)	9.87(−2)	4.6(−8)	6.4(−06)	7.7(−06)	8.2(−06)	1.3(−9)

[a] Wiese & Fuhr 1999, NIST Atomic Spectra Database, National Institute of Standards and Technology (http://physics.nist.gov).
[b] Buurman et al. 1986.
[c] TOPbase.

1998a). The values listed in the VALD database are consistently lower, by factors 2–3. In particular, for the resonance lines they are half the value given by Anstee & O'Mara (1995), which, as we will show below, results in a good fit to the observations.

Collisional excitation rates are given by

$$C_{lu} = n_e \Omega_{lu}(T) \exp(-h\nu_{ul}/kT) \ . \quad (4)$$

Our values for $\Omega_{lu}(T)$ are given in Tables 2 and 3 for the optically allowed and forbidden transitions, respectively.

The rates for the allowed transitions were computed using Van Regemorter's (1962) formula. The forbidden transitions, on the other hand, were computed assuming an Einstein coefficient of 10^5 s^{-1} and using Van Regemorter's formula.

Collisions with atomic hydrogen have been proposed as an important process to take into account for profile synthesis, in particular for cool stars. For example, Lemke & Holweger (1987) included them in studies of Mg I lines. Andretta, Doyle, & Byrne (1997) also considered collisions with H in their calculation of Na D profiles in dM stars, although they found that the effect of these collisions is not important for the emerging profiles.

BG96 included collisions with H in their study of the Al lines and found that the lines are "only marginally affected by hydrogen collisions." Since they used an atmospheric model with no chromosphere, and therefore with lower temperatures than ours, this effect should be even less important in our case. In effect, collisions with hydrogen are more important for lower temperatures, where the ionization of hydrogen is smaller and $N_{\rm H}/N_e$ is larger.

Anyway, to test whether hydrogen collisions affect the profiles of the resonance lines, we included the corresponding rates expressed as a function of temperature as in equation (4), with $\Omega^{\rm H}_{lu}(T)$ computed as follows. For the allowed transitions, we used the approximation by Drawin (1968), in the generalized form of Steenbock & Holweger (1984), as was done by BG96. The value of $\Omega^{\rm H}_{lu}$(5000 K) for the allowed transitions is included in Table 2.

For forbidden transitions, BG96 used the formula proposed by Takeda (1992), which is simple a scaling of the rates for collisions with electrons, "assuming the similarity of cross sections for both cases." This, however, is a gross overestimation, since cross sections with electrons are much larger than with neutral hydrogen, due to the long-range nature of Coulomb interactions (Mihalas 1970). To be consistent with our treatment of electron collisions for forbidden transitions, we used the same expression than for the allowed ones, with a value of $A_{ul} = 10^5$ s^{-1}. The value of $\Omega^{\rm H}_{lu}$ (5000 K) for the forbidden transitions is shown in Table 3.

Caccin et al. (1993), studied the formation of Na and K lines in sunspot umbra, which should be the ideal testing ground for collisions with hydrogen, due to the low temperatures. They concluded that Drawin's cross sections may be severely overestimated, based both in a fit to the observed profiles and in calculations by Kaulakys (1985, 1986). We will return to this point in § 5.2.

Thus, the collisional rates are, at best, rough estimates. Since collisional processes affect the solution of the statistical equilibrium equations in an indirect way, except in the deep atmosphere where the atom is in LTE, we feel that the results obtained in this work have a greater reliability than such collision-rate uncertainties. We discuss this point further in § 4.

TABLE 3

Atomic Parameters for Nonradiative Bound-Bound Transitions

	Ω_{lu} (cm^3 s^{-1})			$\Omega^{\rm H}_{lu}$ (cm^3 s^{-1})
Line	3000 K	5000 K	8000 K	5000 K
2–1	3.7(−02)	3.4(−02)	3.1(−02)	7.2(−3)
4–1	1.6(−10)	2.0(−10)	2.1(−10)	1.0(−13)
6–1	5.2(−11)	6.0(−11)	6.7(−11)	3.0(−14)
9–1	2.6(−11)	2.6(−11)	3.3(−11)	1.3(−14)
10–1	5.6(−11)	5.6(−11)	7.0(−11)	2.7(−14)
4–2	8.2(−11)	1.0(−10)	1.0(−10)	5.1(−14)
6–2	2.7(−11)	3.0(−11)	3.4(−11)	1.5(−14)
9–2	1.3(−11)	1.3(−11)	1.7(−11)	6.5(−15)
10–2	2.8(−11)	2.8(−11)	3.5(−11)	1.4(−14)
4–3	3.0(−07)	3.2(−07)	4.2(−07)	8.3(−10)
5–3	2.9(−08)	2.6(−08)	2.9(−08)	3.8(−11)
7–3	6.9(−10)	7.0(−10)	7.4(−10)	6.5(−13)
8–3	2.5(−09)	2.4(−09)	2.7(−09)	2.1(−12)
10–3	1.9(−09)	1.9(−09)	2.1(−09)	1.5(−12)
11–3	2.3(−10)	2.3(−10)	2.5(−10)	1.7(−13)
5–4	6.6(−08)	7.0(−08)	8.9(−08)	2.0(−10)
6–4	2.2(−08)	2.4(−08)	3.1(−08)	6.1(−11)
7–4	3.9(−10)	4.4(−10)	4.9(−10)	5.3(−13)
8–4	1.3(−09)	1.4(−09)	1.5(−09)	1.5(−12)
9–4	4.9(−10)	5.1(−10)	5.2(−10)	5.0(−13)
10–4	8.4(−10)	8.5(−10)	9.0(−10)	7.9(−13)
11–4	9.5(−11)	9.4(−11)	1.0(−10)	8.5(−14)
7–5	3.0(−09)	3.3(−09)	3.5(−09)	5.9(−12)
8–5	6.9(−09)	7.3(−09)	7.9(−09)	1.1(11)
11–5	3.2(−10)	3.5(−10)	3.7(−10)	3.7(−13)
9–6	4.4(−09)	4.6(−09)	5.2(−09)	6.6(−12)
10–6	6.0(−09)	6.8(−09)	7.5(−09)	8.5(−12)
8–7	1.7(−05)	1.8(−05)	1.9(−05)	1.3(−7)
10–7	4.0(−07)	4.2(−07)	5.5(−07)	1.1(−9)
11–7	2.6(−08)	3.0(−08)	3.6(−08)	6.3(−11)
11–8	1.8(−08)	2.0(−08)	2.5(−08)	5.7(−11)
10–9	1.5(−05)	1.6(−05)	1.7(−05)	1.5(−7)
11–10	2.1(−06)	2.3(−06)	2.5(−06)	2.8(−8)

3. THE INFLUENCE OF THE DIFFERENT LEVELS

In this section we study the influence of the different levels on the emitted profiles of the 3–1 and 3–2 transitions, at 3944 and 3962 Å, respectively. To do so, we compute the profile of this line for model C of Vernazza, Avrett, & Loeser (1981), as modified in the temperature minimum region by Avrett (1985, see also Maltby et al. 1986) and compare it with the observations reported in the FTS atlas of disk-center intensity by Brault and Neckel (Neckel 1999). The T versus z distribution of the model we use is shown in Figure 3*a*, for the lowest part of the atmosphere, which is of interest here.

The calculations were done using the computer code Pandora, kindly provided by E. H. Avrett (see Avrett & Loeser 1992 for an explanation of the program). An important feature that must be taken into account in every profile synthesis is the line-blanketing due to a very large number of weak atomic and molecular lines. This effect is particularly important in the spectral region where the Al resonance lines are found, where there is such a large number of lines that it is not possible to determine the intensity of the "true continuum." In this work we included the 58×10^6 atomic and molecular lines computed by Kurucz (1991), in the way

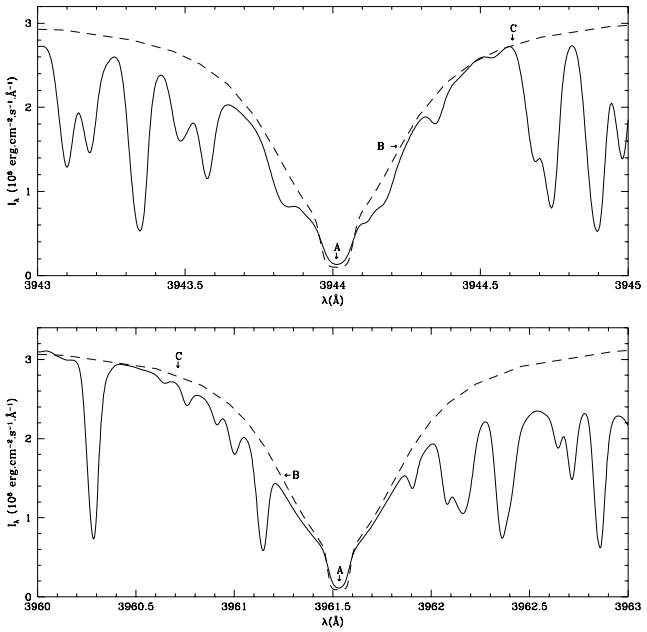

FIG. 2.—Computed (*dashed line*) and observed (*solid line*) profiles. The arrows indicate the wavelengths for which the height of formation is shown in Figs. 3*b* and 3*c*.

explained in Avrett, Machado, & Kurucz (1986) and in Falchi & Mauas (1998).

In Figure 2 we show the computed profiles for both lines and compare them with the observations. It can be seen that the agreement between computed and observed profiles is very good. We point out that this is not a "clean" spectral region, and the lines are in the wings of the very broad Ca II H and K lines, at 3933 and 3968 Å. It can be seen that there are also a large number of weak lines contributing to the line blanketing, a fact that makes it difficult to determine the continuum level.

In Figures 3*b* and 3*c* we show the line source function and the Planck function for the 3944 and 3962 Å lines, which correspond to transitions 3–1 and 3–2, respectively. We also show the depth of formation of the radiation at different wavelengths from line center, marked with arrows in Figure 2. These depths of formation are given for two different values of $\mu\,(=\cos\Theta)$.

It can be seen that the center of both lines form at around 1000 km at disk center, although since the source function at this depth is decoupled from the Planck function, the information given by the line profiles cannot be easily interpreted and depends on the structure of the temperature minimum region.

In Figure 3*d* we show the departure coefficients b_l for the three lowest levels, which are the ones involved in the transitions under study, and for level 9, as an example of the behavior of the highest levels. The departure coefficients are defined such that $n_l/n_k = b_l\, n_l^*/n_k^*$.

Levels 1 and 2 are strongly coupled, since they belong in fact to the same term. The *b*-values for these levels become slightly lower than 1 at first, just below $T_{\min}$, indicating an underpopulation of the levels. Therefore, the source functions for the resonance lines, which can be approximated as

$$S_\nu = \frac{b_3}{b_l} B_\nu \quad (l = 1,\ 2)\ , \tag{5}$$

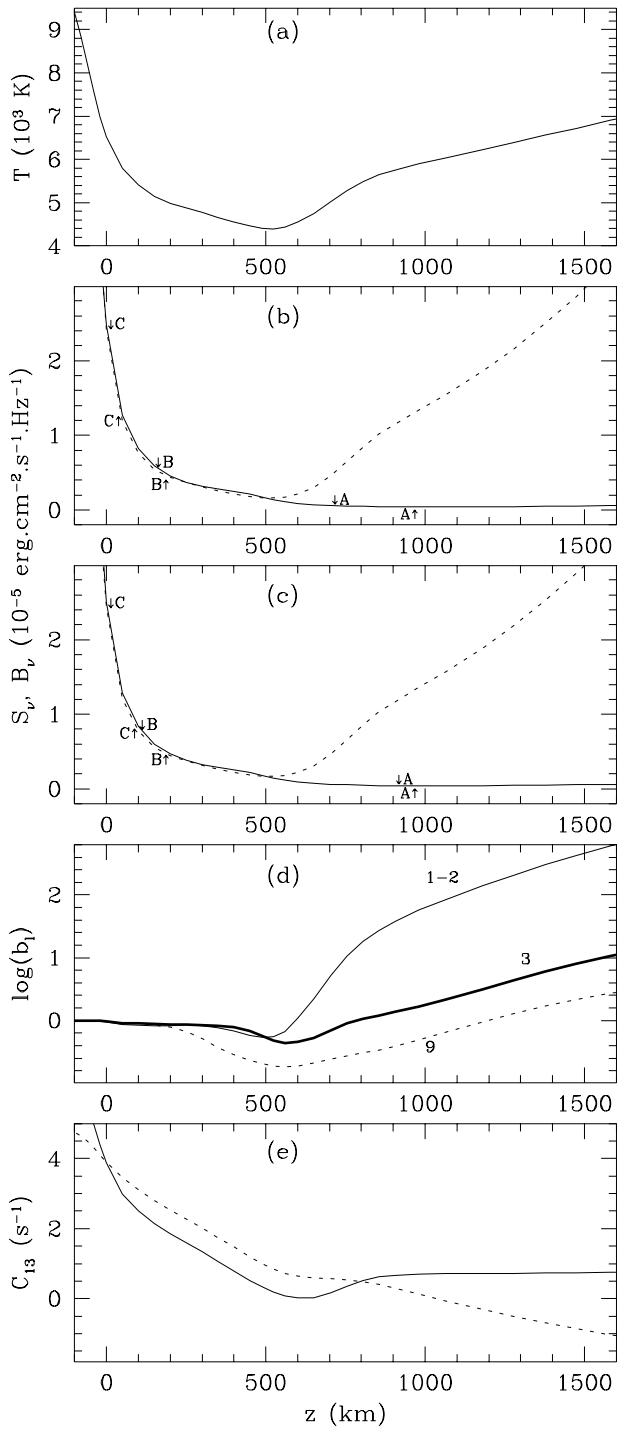

FIG. 3.—(*a*) Atmospheric model used here. (*b*) Source (S_ν, *solid line*) and Planck (B_ν, *dotted line*) functions for the 3–1 transition at 3944 Å. The arrows show the height of formation of the radiation at the wavelengths indicated in Fig. 2. The values at disk center are indicated above the S_ν curve, and those at $\mu = 0.4$ are indicated below it. (*c*) Same as (*b*), for the 3–2 transition at 3961 Å. (*d*) Departure coefficients b_l for several levels. Note that $b_2 = b_1$. (*e*) Collision excitation rates for the 3–1 transition. *Solid line*: collisions with electrons. *Dotted line*: collisions with hydrogen.

become larger than the Planck functions at these heights. Where the line centers are formed, on the other hand, these levels are largely overpopulated, much more than level 3, the upper level of the lines under consideration, and the source function lies below the Planck function.

The ionization equilibrium of Al I in the chromosphere is determined by ionization from the two lowest levels, and recombination to the highest ones, as can be seen in Figure 4. In this figure we show $\mathscr{R}_{lk}$, the net rate of ionization from level l as a function of depth, normalized (for convenience in plotting) by the factor b_1/n_1. $\mathscr{R}_{lk}$ is, therefore, defined as

$$\mathscr{R}_{lk} = (n_l R_{lk} - n_k R_{kl})\ b_1/n_1\ , \qquad (6)$$

where b_1 is the departure coefficient for the ground level, and R_{lk} and R_{kl} are the photoionization and photorecombination rates.

The behavior of the departure coefficient of the ground state shown in Figure 3*d* is similar to the one obtained by BG96, who found an underpopulation of this level in the deep photosphere up to $\tau_{5000} \simeq 2.51 \times 10^{-2}$, with a minimum value of b_1 of around 0.95. However, we found that this effect is larger, since we obtain values of b_1 as low as 0.55, and the underpopulation persists up to $z = 600$ km, which corresponds to $\tau_{5000} \simeq 7 \times 10^{-5}$. This difference can be due to two factors. On one hand, the value we use for the cross sections of the ground levels is a 20% larger than the values they seem to have used, based on an earlier version of TOPbase. On the other, their calculations are for an atmospheric model with no chromosphere, and therefore the UV radiation ionizing the ground level should be lower.

As pointed out in § 2, BG96 used a 51-level atomic model and found in particular that "an effective cascade of infrared transitions including levels 6*h*–5*g*–4*d*–4*p*–4*s* [connects] the $4s\ ^2S$ level efficiently to the highly excited levels and the continuum."

To check whether these additional terms have an influence on the population of the three lowest levels, in particular the $4s\ ^2S$ level (our level 3), and therefore on the emitted line profiles, we made a test run with a model including the 25 terms up to $n = 7$. The transitions involving the new levels are marked as dotted in Figure 1.

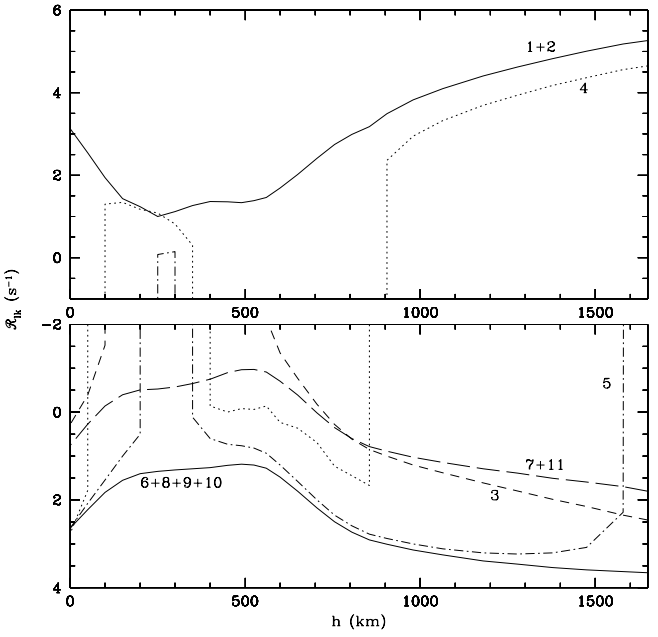

FIG. 4.—Net photoionization rate $\mathscr{R}_{lk}$ for several levels of the atomic model. A positive rate implies net ionization, and a negative rate implies net recombination. For clarity, we group the levels having similar $\mathscr{R}_{lk}$.

We found, indeed, that with the larger number of levels the population of level 3 is increased by as much as 15% in the $T_{\min}$ region and in the low chromosphere. This effect, however, is smaller higher up in the atmosphere and does not affect the profile of the resonance lines, implying that we can continue to use the 11-level model. The effect, on the other hand, is larger in the higher levels, stressing the fact that a model with more levels should be used to compute other lines.

4. THE OPTIMUM MODEL

Since the present atomic model will be used for chromospheric modeling, and in particular to study the velocity fields in the chromosphere, it is very important to find a valid approximation that includes the minimum possible number of transitions, to avoid large computing times.

For each spectral line considered, the transfer equation has to be solved for a number of frequencies, typically of around 30. When the velocity fields are included, the number of frequencies is automatically doubled, since the lines are not symmetric any more. Furthermore, since the frequencies are Doppler shifted by a different amount at each depth, the number of frequencies to work with increases by an additional factor of n, the number of depth points in the grid.

We therefore tried different models with reduced numbers of transitions and found that if we included only the lines with Einstein coefficients $A_{ul} > 10^7\ \mathrm{s}^{-1}$, thus retaining only nine of the original 23 transitions, the profiles for the two lines of interest were not altered, and the computing time was reduced by 25%.

On the other hand, we compute the bound-free rates integrating on a fixed number of wavelengths, which are the same for all levels. Therefore, the number of levels is not as important in determining the computing time as the number of lines.

For example, we made a calculation with a 10-level atomic model, not including level 11 of the standard model. We expected that this change would not affect our calculations since, on one hand, the net ionization rate for this level can be neglected compared to the rates to the other levels and, on the other, all the transitions coupling this level to other levels have $A_{ul} < 10^7\ \mathrm{s}^{-1}$ and can therefore be neglected. The calculations with this 10-level model gave, indeed, the same results than before, but the gain in computing speed was of only 3%. We feel that, in view of this fact, it is not worth reducing the number of levels.

In this way, we arrive to what can be called an "optimum model," in the sense that it includes all the atomic processes that can affect the profiles of the lines under study, being at the same time the one with the smallest number of transitions needed, and thus the fastest to compute. The lines not included in this model are the ones marked with dashed lines in Figure 1, and with an asterisk (*) in Table 2.

5. INFLUENCE OF THE ATOMIC PARAMETERS

We have investigated the influence that a change of the different atomic parameters has either on the computed populations of the atomic levels or on the profiles of the lines under study, as a way to estimate how the uncertainty

on these parameters is reflected in the computed profiles. The results of these calculations are presented in this section.

5.1. *Photoionization Cross Sections*

As pointed out in § 2.1, the photoionization cross sections adopted here are theoretical values, and, as far as we are aware, the only experimental values for these parameters are for the ground state. Therefore, we paid particular attention to how errors in these cross sections can affect the emitted profiles.

Since, as can be seen in Figure 4, the two lowest levels are the most important for the ionization and are the two lower levels for the transitions under study, we first increased the cross sections for these levels by 2, a factor larger than the uncertainty in this parameter. We found that this produced an increase of around 15% in the ionization of Al I around 1000 km, where the line centers are formed, and of less than 10% in the minimum value of b_1, in the photosphere where the ground state is underpopulated.

However, the relative equilibrium between the bound levels does not change so much, and the source function is about 7% lower in this case. The line center intensity changes even less, being 3% lower. However, even this amount is misleading, since the line is so deep. If the line depth is considered, the change is completely negligible.

We made other runs, changing the cross sections for levels 8, 9, and 10 by factors of 2 in either sense, but in this case the changes in ionization are even smaller, of less than 3%. If the cross sections for levels 5 and 6 are increased by a factor of 2, the ionization at the height where the lines are formed decreases by 7%, but also in this case the effect in the line profiles can be neglected. Changes in the remaining cross sections have no consequences, since the levels are irrelevant for the ionization equilibrium, as can be seen in Figure 4.

The fact that these lines are not affected by these changes in the cross sections is an advantage when using the profiles as chromospheric diagnostics, since the conclusions are not affected by indeterminations in the atomic parameters. Furthermore, since the opacity sources, especially in the UV, are not known very precisely, there is also an important indetermination in the continuum level at these wavelengths (see, e.g., Bell, Balachandran, & Bautista 2001 for a reassessment of Fe I opacities). Since the photoionization rate is given by the convolution of the cross section with the continuum intensity, we can conclude that the line profiles are not sensitive to reasonable changes in the continuum radiation.

5.2. *Collisional Cross Sections*

As explained in § 2, the collisional cross sections are the parameters in these calculations that have the largest uncertainties. To assess the importance of this indetermination in the computed profiles, in this section we explore the influence that variations on the collisional rates can have on the observed profiles.

We first increased by a factor of 10 the collisional ionization cross sections for the first two levels and found that the changes in the degree of ionization staid below 2% everywhere. We also tried increasing by the same amount the cross sections for levels 3, 5, and 6. In this case there was a decrease in the population of level 3 in the region around $T_{\rm min}$, which never exceeded 5% and did not affect the line profiles. Finally, we multiplied by 10 the rates from levels 4 and 7 to 11, which were rough estimates. The effect in this case was even smaller.

We then increased by a factor of 5 the collision rates between level 3 and the two lowest levels. This brought the source function closer to the Planck function in the region where the former is larger, around 350 km. However, it did not affect the source function where the line center is formed, and therefore it did not affect the profiles. A similar result is obtained by increasing the 4–3 collision rate.

We also tried increasing by 5 the excitation rates of the two ground states to all the higher ones (except level 3) and found that the influence on the level populations was negligible. If the excitation rates of level 3 to the others is increased by the same factor, the b_3 is slightly smaller throughout the chromosphere, but this does not change the line profiles noticeably.

One of the less reliable approximations we made was to set the cross sections for nonradiative bound-bound transitions equal to the ones for an allowed transition with the same energy difference and a value of the Einstein coefficient $A_{ul} = 10^5$ s^{-1}. In a study of the Mg I lines, Mauas, Avrett, & Loeser (1988) computed these cross sections assuming a fixed oscillator strength of 0.1 in Van Regemorter's formula, instead of a fixed value for the Einstein A_{ul}. This criterion results in larger values for the collision rates between levels with smaller energy difference. If this is done, the populations of the highest levels are brought closer to LTE, but the profiles of the resonance lines are not affected.

As was mentioned in § 2.2, there is a large uncertainty about the importance of collisions with hydrogen in the statistical equilibrium of different elements. To investigate its importance in this case, in Figure 3*e* we plot the excitation rate for one of the resonance lines, the 3–1 transition, both for collisions with electrons and for collisions with hydrogen. It can be seen that the rates for hydrogen are indeed larger in the photosphere and up to the $T_{\rm min}$.

However, in most of that region the lines are very close to LTE, and the only effect of the inclusion of the hydrogen rates is to bring the source functions closer to the Planck function in the region between 300 and 500 km. Higher up in the atmosphere, even in the regions where collisions with hydrogen are larger than with electrons, other processes are more important for the statistical equilibrium, and the source function is not affected. The profiles of the resonance lines, therefore, remain unchanged.

Taking into consideration that Drawin's cross sections, which we use in this paper, are most probably large overestimates, we feel confident that collisions with hydrogen can be neglected when computing the profiles of the resonance lines. They can, in principle, be important for other lines, which we did not investigate here. However, since weaker lines form deeper in the atmosphere, where the populations are closer to LTE, the inclusion of larger collision rates should not affect the line profiles too much.

5.3. *The Einstein Coefficients*

The Einstein coefficients of the lines under study have, in principle, a strong influence on the computed profiles, since they determine the depth of formation of the line.

As explained in § 2.2, the values of the A_{ul} found in the literature for the lines under study differ by 10% between the maximum and minimum values. The value adopted here is

between those values, and therefore the indetermination is lower. However, since such a good agreement can be due to the scarcity of work on the subject, we made a trial run with the A_{ul} for both lines incremented by 20%. This causes the line center to be formed higher in the chromosphere. However, it can be seen in Figure 3 that the source functions for both lines are very flat in this region, and therefore the central intensities are not modified at all.

On the other hand, moving outward the region of formation of the line center implies that the computed profile turns out slightly wider. It is possible to compensate this effect changing the Van der Waals width of the lines: if $C_{\rm VdW}$ is reduced from 1.5 to 1.3×10^{-4} Å, the profiles result is identical to the original ones. However, since the values we use for $C_{\rm VdW}$ give a good fit to the observations, we find that the present result is a good confirmation of both the A_{ul} and the $C_{\rm VdW}$ for these transitions.

We also tried incrementing by 20% the A_{ul} of the transitions "feeding" the lower levels of the transitions under study (i.e., the transitions from levels 5, 7, 8, and 11 to levels 1 and 2), which did not affect the profiles. A similar result was obtained when the A_{ul} for transitions 6–3 and 9–3 were incremented by 20%.

5.4. *Damping Parameters*

We have found that Van der Waals broadening is the main factor in determining the Voigt parameter (eq. [3]) in the region of formation of the lines under study. As can be seen in Figure 2, the value we use provides a good fit to the width of the resonance lines. As was explained in § 2.2, the VALD database gives values smaller than the ones used here. We tried VALD's values for all the lines except the ones for transitions 3–1 and 3–2, and the computed profiles for these lines remain the same.

BG96 did a semiempirical fit of the Van der Waals widths, for all the lines they study. For the resonance transitions, their value corresponds to that of $C_{\rm VdW} = 4.5 \times 10^{-4}$ Å, 3 times ours.

Increasing the Van der Waals widths by a 30% increases the equivalent widths of the lines by 10%, from 0.9 to 1 Å for the 3966 Å line and from 0.63 to 0.70 Å for the 3944 Å line. Stark broadening, on the other hand, is less important, although not completely negligible, and the same 10% increase in the equivalent width can be obtained multiplying the $C_{\rm Stk}$ by a factor of 10.

5.5. *Opacities*

Although rather insensitive to variations in the Al I atomic parameters, the line profiles are strongly dependent on the sources of continuum opacities included in the calculations. Here we have considered, in addition to Rayleigh and electron scattering, the absorptions due to H^-, H, H^{2+}, He, He II, Mg, C, Si, Fe, Na, and Ca as well as Al itself, and all these contributions were obtained from non-LTE computed populations. As explained in § 3, we have also included the contribution due to weak atomic and molecular lines compiled by Kurucz (1991) in the way explained by Falchi & Mauas (1998).

As this method treats the opacity in a statistical way, it is appropriate to compute the photoionization rates, which depend on the integral of the radiation, and to give an approximate idea of the continuum level but does not reproduce the exact radiation field at a precise wavelength.

In particular, both lines under study lie in the wings of the Ca II H and K lines, and therefore the "continuum" level the lines see is determined by the Ca lines, and not by continuum absorption. Here we had to adjust the opacity to fit the intensity in the wings of the line. It should also be noted that this intensity is different for both lines and is even different at both sides of the same line, something we could not reproduce.

Although these continuum opacities, and the ad hoc adjustments we had to make, do not affect the intensity at line center, it does affect the residual intensity, because it changes the continuum level. For these lines, the continuum obtained without adjusting for Ca II absorption is 25% higher. Therefore, residual intensities should be used with caution when comparing with the observations. For a more thorough discussion of this and other effects that can affect the atmospheric modeling, see Falchi & Mauas (1998).

To study the influence of these weak-line opacities in the ionization of Al I, we recomputed the model using the average line opacity distribution of VAL II in the ionization continua of the lowest levels, in an approach similar to the one used by BG96. This produced an increase of the recombination rates and a decrease of the ionization rates, leading to a decrease in the overall ionization of as much as 40% in the chromosphere. This effect is similar to the case of Mg I studied by Mauas et al. (1988) and different to the case of Si I studied by CM01, where the differences were smaller than 5%.

However, since the balance between the populations of the bound levels is not affected, the source function remained almost unaltered, and the profiles did not change at all.

6. LINE IRRADIATION

CM01 found that the ionization balance of Si I can be strongly affected by the irradiation from ultraviolet lines coming down from the upper chromosphere or the transition region and that this irradiation can alter the continuum intensity below 1682 Å, the ionization threshold of level 2 of Si I.

We have studied whether this effect can also be found on Al I ionization, since the ionization threshold is not much larger than the one for Si I. To do this, we have computed the Al I equilibrium assuming the different levels of radiation in the lines listed in Table 4 of CM01, corresponding to plage and sunspot umbra. We also tried an irradiating flux equal to 10^3 times the one used for the plage, a level that can be considered representative of the situation during flares.

Only in this last case the ionization balance was slightly affected, but changes in the continuum emission were very small, and the line profiles remained unaltered.

7. CONCLUSIONS

We have compiled a reliable atomic model for profile calculations of the two resonance lines of Al I in the blue region of the spectrum. We found that, since these lines affect the lowest levels, only 11 levels are necessary. Furthermore, it is not necessary to explicitly compute the radiative transitions for all the lines between these levels, and a model much faster to compute can be obtained considering only nine of the strongest lines.

We have studied the influence that the uncertainties in the values of the different atomic parameters may have on the calculated profiles and have found that both profiles are rather insensitive to these parameters, within the reasonable values to be expected. This characteristic is very important, since it makes these lines very reliable as chromospheric diagnostics.

We have also assessed the importance of considering the line-blanketing for the ionization balance and have found that the opacity due to the wings of Ca II needs to be properly taken into account, in particular if the profiles are to be considered in residual intensity.

On the other hand, we found that the Al I continua and the lines under study are not sensitive to the irradiation by ultraviolet lines originating in the transition region.

We stress that these results apply only to the calculation of the resonance line profiles, since when computing lines connecting higher levels the effects we studied could be different.

REFERENCES

Andretta, V., Doyle, J. G., & Byrne, P. B. 1997, A&A, 322, 266
Anstee, S. D., & O'Mara, B. J. 1995, MNRAS, 276, 859
Avrett, E. H. 1985, in Chromospheric Diagnostics and Modeling, ed. B. W. Lites (Sunspot: NSO), 67
Avrett, E. H., & Loeser, R. 1992, ASP Conf. Ser. 26, Cool Stars, Stellar Systems, and the Sun: Seventh Cambridge Workshop, ed. M. S. Giampapa & J. A. Bookbinder (San Francisco: ASP), 489
Avrett, E. H., Machado, M. E., & Kurucz, R. L. 1986, in The Lower Chromosphere of Solar Flares, ed. D. F. Neidig (Sunspot: NSO), 216
Barklem, P. S., Anstee, S. D., & O'Mara, B. J. 1998a, Publ. Astron. Soc. Australia, 15, 336
Barklem, P. S., & O'Mara, B. J. 1997, MNRAS, 290, 102
Barklem, P. S., O'Mara, B. J., & Ross, J. E. 1998b, MNRAS, 296, 1057
Baumüller, D., & Gehren, T. 1996, A&A, 307, 961 (BG96)
———. 1997, A&A, 325, 1088
Bell, R. A., Balachandran, S., & Bautista, M. 2001, ApJ, 546, L65
Buurman, E. P., et al. 1986, A&A, 224, 226
Caccin, B., Gomez, M. T., & Severino, G. 1993, A&A, 276, 219
Cauzzi, G., et al. 1995, A&A, 299, 611
Cincunegui, C., & Mauas, P. J. D. 2001, ApJ, 552, 877 (CM01)
Cunto, W., et al. 1993, A&A, 275, L5
Dragon, J. N., & Mutschlecner, J. P. 1980, ApJ, 239, 1045
Drawin, H. W. 1968, Z. Phys., 211, 404
Falchi, A., & Mauas, P. J. D. 1998, A&A, 336, 281
———. 2002, A&A, 387, 678
Grevesse, N., et al. 1991, A&A, 242, 488
Kaulakys, B. 1985, J. Phys. B, 18, L167
Kaulakys, B. 1986, Soviet Phys, JEPT, 64, 229
Kohl, J. L., & Parkinson, W. H. 1973, ApJ, 184, 641
Kupka, F., Piskunov, N. E., Ryabchikova, T. A., Stempels, H. C., & Weiss, W. W. 1999, A&AS, 138, 119
Kurucz, R. L. 1991, in Precision Photometry: Astrophysics of the Galaxy, ed. A. G. Davis Philip, A. R. Upgren, & K. A. Janes (Schenectady: Davis), 27
Lemke, M., & Holweger, H. 1987, A&A, 173, 375
Linsky, J. L., Hunten, D. M., Sowell, R., Glackin, D. L., & Kelch, W. L. 1979, ApJS, 41, 481
Maltby, P., et al. 1986, ApJ, 306, 284
Mauas, P. J. D., Avrett, E. H., & Loeser, R. 1988, ApJ, 330, 1008
Mendoza, C., Eissner, W., Le Dourneuf, M., & Zeippen, C. J. 2002, in press
Mihalas, D. 1970, Stellar Atmospheres (San Francisco: Freeman)
Morton, D. C. 1991, ApJS, 77, 119
Neckel, H. 1999, Sol. Phys., 184, 421
Peach, G. 1970, MNRAS, 73, 1
Piskunov, N. E., Kupka, F., Ryabchikova, T. A., Weiss, W. W., & Jeffery, C. S. 1995, A&AS, 112, 525
Roig, R. A. 1975, J. Phys. B, 8, 2939
Röndings, G., & Kush, H. J. 1978, A&A, 70, 151
Ryabchikova, T. A., et al. 1999, Phys. Scr., 83, 162
Steenbock, W., & Holweger, H. 1984, A&A, 130, 319
Takeda, Y. 1992, A&A, 242, 455
Van Regemorter, H. 1962, ApJ, 136, 906
Vernazza, J. E., Avrett, E. H., & Loeser, R. 1976, ApJS, 30, 1
———. 1981, ApJS, 45, 635